Nguyen Thanh Phuong, Ho Dac Loc, Tran Quang Thuan / International Journal of Engineering Research and Applications (IJERA) ISSN: 2248-9622 www.ijera.com
Vol. 3, Issue 3, May-Jun 2013, pp.1276-1282

Control of Two Wheeled Inverted Pendulum Using Silding Mode Technique

Nguyen Thanh Phuong, Ho Dac Loc, Tran Quang Thuan
Ho Chi Minh City University of Technology (HUTECH) Vietnam

Abstract

In this paper, a controller via sliding mode control is applied to a two-wheeled inverted pendulum, which is an inverted pendulum on a mobile cart carrying two coaxial wheels. The controller is developed based upon a class of nonlinear systems whose nonlinear part of the modeling can be linearly parameterized. The tracking errors are defined, then the sliding surface is chosen in an explicit form using Ackermann's formula to guarantee that the tracking error converge to zero asymptotically. The control law is extracted from the reachability condition of the sliding surface. In addition, the overall control system is developed. The simulation and experimental results on a two-wheel mobile inverted pendulum are provided to show the effectiveness of the proposed controller.

Key-Words: - *Sliding mode controller, two wheeled inverted pendulum.*

1 Introduction

The two-wheeled inverted pendulum is a novel type of inverted pendulum. In 2000, Felix Grasser et al. [1] built successfully a mobile inverted pendulum JOE. SEGWAY HT was invented by Dean Kamen in 2001 and made commercially available in 2003. The basic concept was actually introduced by Prof. Kazuo Yamafuzi in 1986.

In practice, various inverted pendulum systems have been developed. Inverted pendulum systems always exhibit many problems in industrial applications, for example, nonlinear behaviors under different operation conditions, external disturbances and physical constraints on some variables. Therefore, the task of real time control of an unstable inverted pendulum is a challenge for the modern control field.

Chen et al. [2] proposed robust adaptive control architecture for operation of an inverted pendulum. Though the stability of the control strategies can be guaranteed, some prior knowledge and constraints were required to ensure the stability of the overall system. Huang et al. [3] proposed a grey prediction model combined with a PD controller to balance an inverted pendulum. The control objective is to swing up the pendulum from a stable position to an unstable position and to bring its slider back to the origin of the moving base. However, the stability of this control scheme cannot be assured.

On the other hand, there are many literatures on sliding mode control theory, which is one of the effective nonlinear robust control approaches. Juergen et al. [4] designed a sliding mode controller based on Ackermann's Formula. Their simulation results prove that the mobile inverted pendulum can be balanced by this controller. There is no tracking controller. So tracking controller of mobile inverted pendulum is deeply needed.

In this paper, a practical controller via sliding mode control is applied to control two-wheeled mobile inverted pendulum. The sliding surface is chosen in an explicit form using Ackermann's formula, and the control law is extracted from the reachability condition of the sliding surface [5]. Finally, the simulation and experimental results on computer are presented to show the effectiveness of the proposed controller.

The two-wheeled mobile inverted pendulum prototype is shown in Fig. 1. It is composed of a cart carrying a DC motor coupled to a planetary gearbox for each wheel, the microcontroller used to implement the controller, the incremental encoder and tilt sensor to measure the states, as well as a vertical pendulum carrying a weight.

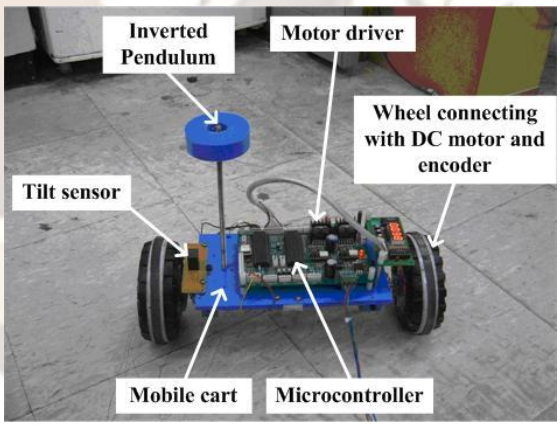

Fig. 1 Two-wheeled mobile inverted pendulum

2 System Modelling

In this paper, it is assumed that the wheels always stay in contact with the ground and that there will be no slip at the wheel's contact patches.

The motor dynamics have been considered [5]. Fig. 2 shows the conversion of the electrical energy from the DC power supply into the mechanical energy supplied to the load.

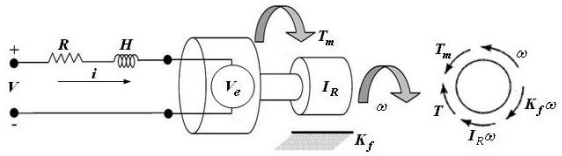

Fig. 2 The diagram of DC motor

The motor model is given as follows [6],

$$T_m = \frac{K_m}{R}V - \frac{K_m K_e}{R}\omega \quad (1)$$

Parameters are given in Appendix A.

Straight Motion Modeling

In straight motion modeling of mobile inverted pendulum, the left and right wheels are driven under identical velocity, i.e., $\dot{x}_l = \dot{x}_R = \dot{x}_r$.

The modeling can be linearized by assuming $\varphi = \phi$, where ϕ represents a small angle from the vertical direction,

$$cos\,\varphi = 1, sin\,\varphi = \phi, \left(\frac{d\varphi}{dt}\right)^2 = 0 \quad (2)$$

The dynamics equation in the straight motion is as follows [6],

$$\dot{x} = Ax + bu \quad (3)$$

$$A = \begin{bmatrix} 0 & 1 & 0 & 0 \\ 0 & a_{22} & a_{23} & 0 \\ 0 & 0 & 0 & 1 \\ 0 & a_{42} & a_{43} & 0 \end{bmatrix}, x = \begin{bmatrix} x_r \\ \dot{x}_r \\ \phi \\ \dot{\phi} \end{bmatrix}, b = \begin{bmatrix} 0 \\ b_2 \\ 0 \\ b_4 \end{bmatrix},$$

where $a_{22}, a_{23}, a_{42}, a_{43}, b_2, b_4$ and d are defined as a function of the system's parameters, which are given in Appendix B.

Tracking error is defined as

$$\begin{aligned} e_1 &= x_r - x_d, \\ e_2 &= \dot{x}_r - \dot{x}_d, \\ e_3 &= \phi - \phi_d, \\ e_4 &= \dot{\phi} - \dot{\phi}_d \end{aligned} \quad (4)$$

where x_d is desired value, ϕ_d is desired inverted pendulum angle.

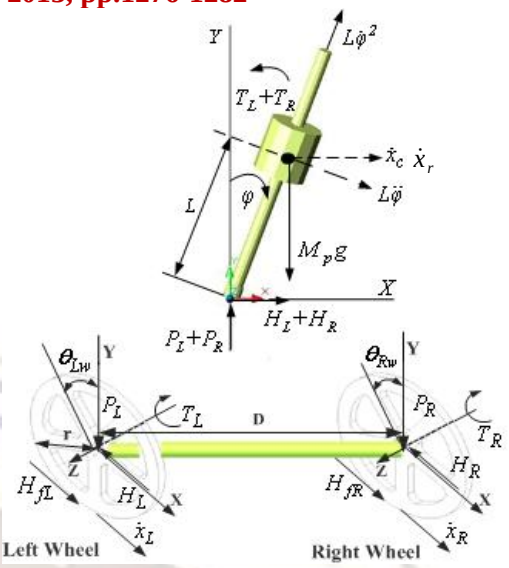

Fig. 3 Free body of motion modeling

From Eq. (4), the followings are obtained.

$$\begin{aligned} x_r &= x_d + e_1 \\ \dot{x}_r &= \dot{x}_d + e_2 = \dot{x}_d + \dot{e}_1 \\ \ddot{x}_r &= \ddot{x}_d + \dot{e}_2 \\ \phi &= \phi_d + e_3 \\ \dot{\phi} &= \dot{\phi}_d + e_4 = \dot{\phi}_d + \dot{e}_3 \\ \ddot{\phi} &= \ddot{\phi}_d + \dot{e}_4 \end{aligned} \quad (5)$$

From Eq. (5), the following can be obtained

$$\begin{aligned} e_2 &= \dot{e}_1 \\ e_4 &= \dot{e}_3 \end{aligned} \quad (6)$$

Substituting Eq. (5) into Eq. (3), the following can be obtained.

$$\begin{bmatrix} \dot{x}_d + \dot{e}_1 \\ \ddot{x}_d + \dot{e}_2 \\ \dot{\phi}_d + \dot{e}_3 \\ \dot{\phi}_d + \dot{e}_4 \end{bmatrix} = A \begin{bmatrix} x_d + e_1 \\ \dot{x}_d + e_2 \\ \phi_d + e_3 \\ \dot{\phi}_d + e_4 \end{bmatrix} + bu \quad (7)$$

Rearranging Eq. (7), the following can be obtained

$$\begin{bmatrix} \dot{e}_1 \\ \dot{e}_2 \\ \dot{e}_3 \\ \dot{e}_4 \end{bmatrix} = A \begin{bmatrix} e_1 \\ e_2 \\ e_3 \\ e_4 \end{bmatrix} + bu + A \begin{bmatrix} x_d \\ \dot{x}_d \\ \phi_d \\ \dot{\phi}_d \end{bmatrix} - \begin{bmatrix} \dot{x}_d \\ \ddot{x}_d \\ \dot{\phi}_d \\ \dot{\phi}_d \end{bmatrix} \quad (8)$$

where

$$A\begin{bmatrix} x_d \\ \dot{x}_d \\ \phi_d \\ \dot{\phi}_d \end{bmatrix} - \begin{bmatrix} \dot{x}_d \\ \ddot{x}_d \\ \dot{\phi}_d \\ \ddot{\phi}_d \end{bmatrix} = \begin{bmatrix} \dot{x}_d \\ a_{22}\dot{x}_d + a_{23}\phi_d \\ \dot{\phi}_d \\ a_{42}\dot{x}_d + a_{43}\phi_d \end{bmatrix} - \begin{bmatrix} \dot{x}_d \\ \ddot{x}_d \\ \dot{\phi}_d \\ \ddot{\phi}_d \end{bmatrix}$$

$$= \begin{bmatrix} 0 \\ a_{22}\dot{x}_d + a_{23}\phi_d - \ddot{x}_d \\ 0 \\ a_{42}\dot{x}_d + a_{43}\phi_d - \ddot{\phi}_d \end{bmatrix} = \begin{bmatrix} 0 \\ d_2 \\ 0 \\ d_4 \end{bmatrix}$$

From Eq. (8), the following error dynamic equation of mobile inverted pendulum is obtained:

$$\dot{e} = Ae + bu + d \quad (9)$$

where $e = \begin{bmatrix} e_1 \\ e_2 \\ e_3 \\ e_4 \end{bmatrix}, b = \begin{bmatrix} 0 \\ b_2 \\ 0 \\ b_4 \end{bmatrix}, d = \begin{bmatrix} 0 \\ d_2 \\ 0 \\ d_4 \end{bmatrix}$.

Rearranging Eq. (9), the following can be obtained

$$\dot{e} = Ae + b\left(u + \tilde{d}\right) = Ae + bu_1 \quad (10)$$

where $u_1 = u + \tilde{d}$.

Proof of Eq. (10)

$$b\tilde{d} = d \quad (11)$$

Because b is not square matrix, the following is obtained by pseudo inverse of b

$$\tilde{d} = \left(b^T b\right)^{-1} b^T d \quad \text{for } \left|b^T b\right| \neq 0 \quad (12)$$

where $b^T b = \begin{bmatrix} 0 & b_2 & 0 & b_4 \end{bmatrix} \begin{bmatrix} 0 \\ b_2 \\ 0 \\ b_4 \end{bmatrix} = b_2^2 + b_4^2$.

If $b_2 = 0$ and $b_4 = 0 (b = 0)$, Eq. (10) is given as

$$\dot{e} = Ae \quad (13)$$

If $b_2^2 + b_4^2 > 0$,

$$\tilde{d} = \left(b^T b\right)^{-1} b^T d = \frac{b_2 d_2 + b_4 d_4}{b_2^2 + b_4^2} \quad (14)$$

In this paper, $b_2^2 + b_4^2 > 0$, x_d and ϕ_d are consider as constant, so

$$\tilde{d} = \frac{b_2 a_{23} + b_4 a_{43}}{b_2 \cdot b_2 + b_4 \cdot b_4} \phi_d \quad (15)$$

where ϕ_d is constant, so $\tilde{d}$ is also constant.

3 Controller Design

The control law u is defined as

$$u_1 = u + \tilde{d} = u_a + u_2 \quad (16)$$

where static controller u_a contributes the design of sliding surface, and dynamic controller u_2 directly makes sliding surface attractive to the system state.

The static system is nominal system as follows:

$$\dot{e} = Ae + bu_a \quad (17)$$

The static controller is given by Ackermann's formula as follows:

$$u_a = -k^T e \quad (18)$$

$$k^T = h^T P(A), h^T = \left[0,0,0,1\right]\left[b, Ab, A^2 b, A^3 b\right]^{-1},$$

$$P(\lambda) = (\lambda - \lambda_1)(\lambda - \lambda_2)(\lambda - \lambda_3)(\lambda - \lambda_4)$$

where $\lambda_1, \lambda_2, \lambda_3, \lambda_4$ are the desired eigenvalues and $P(\lambda)$ is characteristic polynomial of Eq. (17).

Substituting Eq. (18) into Eq. (17), the equation of closed loop system is obtained as

$$\dot{e} = \left(A - bk^T\right)e \quad (19)$$

The sliding surface is chosen as

$$S = C^T e, C^T = h^T P_1(A) \quad (20)$$

where $P_1(\lambda) = (\lambda - \lambda_1)(\lambda - \lambda_2)(\lambda - \lambda_3)$,

$\equiv p_1 + p_2\lambda + p_3\lambda^2 + \lambda^3$.

Proof of Eq. (20)

The left eigenvector C^T of $A - bk^T$ associated with λ_4 satisfies

$$C^T(A - bk^T) = C^T \lambda_4 \quad (21)$$

Rearranging Eq. (21) can be obtained as

$$C^T(A - \lambda_4 I) = C^T bk^T \quad (22)$$

$$C^T b = h^T(A - \lambda_1 I)(A - \lambda_2 I)(A - \lambda_3 I)b \quad (23)$$

$$= \left[0,0,0,1\right]\left[b, Ab, A^2 b, A^3 b\right]^{-1}$$

$$\cdot \left[b \quad Ab \quad A^2 b \quad A^3 b\right]\left[p_1 \quad p_2 \quad p_3 \quad 1\right]^T$$

$$= 1$$

Substituting Eqs. (18), (20) and (23) into Eq. (22) yields

$$k^T = C^T(A - \lambda_4 I) = h^T P_1(A)(A - \lambda_4 I)$$

$$k^T = h^T P(A)$$ □

Substituting Eqs. (16) and (18) into Eq. (10), the dynamic controller as perturbed system is obtained as follows:

$$\dot{e} = (A - bk^T)e + bu_2 \quad (24)$$

A new variable z is defined as

$$z = \begin{bmatrix} e^1 \\ \cdots \\ S \end{bmatrix} = \begin{bmatrix} I & 0 \\ \cdots & \\ C^T & \end{bmatrix} e = Te \quad (25)$$

where $e^1 = \left[e_1, e_2, e_3\right]^T$ is the first three error variables of e and $S = C^T e$ becomes the last state variable of z.

The new coordinate system can be obtained as

$$\dot{z} = T(A - bk^T)T^{-1}z + Tbu_2 = \bar{A}z + \bar{B}u_2 \quad (26)$$

The transformed system is

$$\dot{e}^1 = A_1 e^1 + a_1 S + b^1 u_2 \quad (27)$$

$$\dot{S} = \lambda_4 S + u_2 \quad (28)$$

where $b^1 = [b_1, b_2, b_3]^T$,

$$\bar{A} = T(A - bk^T)T^{-1} = \begin{bmatrix} A_1 & a_1 \\ 0 & \lambda_4 \end{bmatrix}, \bar{B} = Tb = \begin{bmatrix} b^1 \\ 1 \end{bmatrix}.$$

$\bar{A}$ is shown in details in Appendix C

Proof of (28)

Differentiating Eq. (20) and substituting Eqs. (10), (21) and (23), the following can be reduced into

$$\dot{S} = C^T \dot{e} = C^T \left[\left(A - bk^T \right) e + bu_2 \right]$$

$$= C^T \left(A - bk^T \right) e + C^T b u_2$$

$$= \lambda_4 C^T e + u_2 = \lambda_4 S + u_2 \quad (29)$$

The dynamic controller is chosen as

$$u_2 = -M(e,t)\,sign(S) \quad (30)$$

where $M(e,t) > \left| \lambda_4 C^T e \right|$.

Proof of (30)

According to reachability condition $\lim_{S \to 0} S \cdot \dot{S} \le 0$, the followings must be satisfied,

i) $S > 0$ and $\dot{S} < 0$

$$\dot{S} = \lambda_4 C^T e + u_2 < 0$$

$$u_2 < -\lambda_4 C^T e$$

$$-M(e,t)\,sign(S) < -\lambda_4 C^T e$$

$$M(e,t) > \lambda_4 C^T e$$

ii) $S < 0$ and $\dot{S} > 0$

$$\dot{S} = \lambda_4 C^T e + u_2 > 0$$

$$u_2 > -\lambda_4 C^T e$$

$$-M(e,t)\,sign(S) > -\lambda_4 C^T e$$

$$M(e,t) < -\lambda_4 C^T e$$ □

From Eqs. (16) and (18), the control law is given as

$$u = -k^T e + u_2 - \tilde{d} \quad (31)$$

4 Hardware Design

The control system is specially designed for two-wheeled mobile inverted pendulum. The control system is based on the integration of three PIC16F877s: two for servo controllers and one for main controller. The main controller which is functionalized as master links to the two servo controllers, as slave, via I2C communication. The total configuration of the control system is shown in Fig. 4.

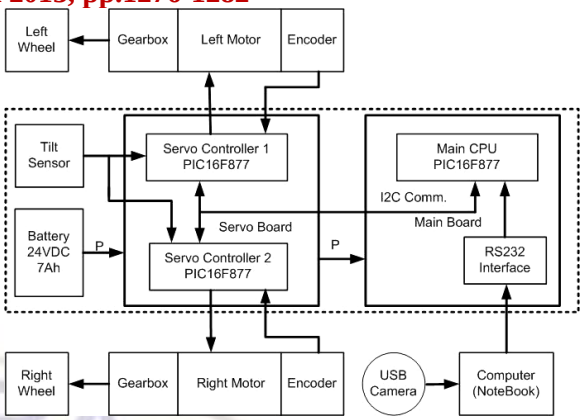

Fig. 4 The configuration of control system

5 Simulation and Experimental Results

The parameters for two-wheeled mobile inverted pendulum used for simulation are given in Table 1.

Table 1 System numerical values

Parameters	Values	Units
r	0.05	m
M_p	1.13	Kg
I_p	0.004	$Kg \cdot m^2$
K_e	0.007	Vs/rad
K_m	0.006	Nm/A
R	3	Ω
M_w	0.03	Kg
I_w	0.001	$Kg \cdot m^2$
L	0.07	m
g	9.8	m/s^2

Substituting system's parameters into Eqs. (24), the state space equation can be rewritten as follows:

$$\dot{e} = \begin{bmatrix} 0 & 1 & 0 & 0 \\ -0.4228 & -0.8809 & -2.1459 & 0.8822 \\ 0 & 0 & 0 & 1 \\ 4.3309 & 9.1060 & -34.5772 & -9.1191 \end{bmatrix} e + \begin{bmatrix} 0 \\ 0.1989 \\ 0 \\ -2.0565 \end{bmatrix} u_2 \quad (32)$$

where $\lambda_1 = -1, \lambda_2 = -2, \lambda_3 = -3, \lambda_4 = -4$.

It is readily shown that the rank of the controllability matrices is full.

Simulation has been done for the proposed controller to be used in the practical field. In addition, the controller was applied to the two-wheeled inverted pendulum for the experiment. It is shown that the proposed controller can be used in the practical field.

In the case of straight motion modeling, the parameters of the sliding surface are

$\lambda_1 = -1$, $\lambda_2 = -2, \lambda_3 = -3$; the parameters of the control law is $M_0 = 40$; the initial values x_r, ϕ are zero, and initial errors are $e_1 = -1.0m$ and $e_3 = -0.1rad$.

Fig. 5 shows that the cart position error has the convergent time of 5 seconds. Fig. 6 shows that the inverted pendulum angle error is bounded around zero after 4 seconds. Fig. 7 shows the sliding surface to converge zero very fast in simulation.

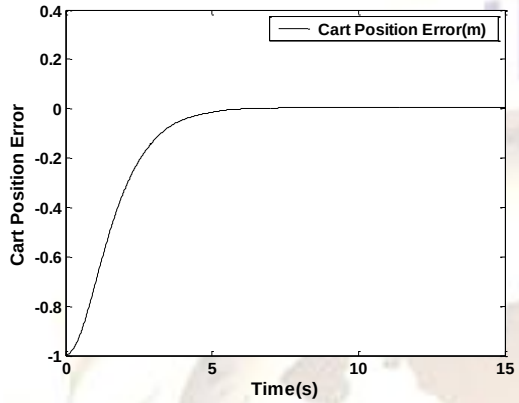

Fig. 5 Cart position error $e_1 = -1.0m$

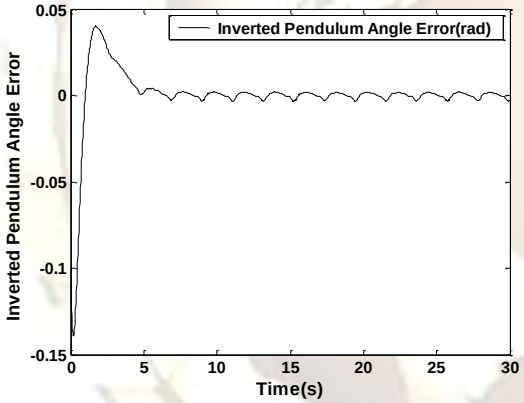

Fig. 6 Inverted pendulum angle error $e_3 = -0.1rad$

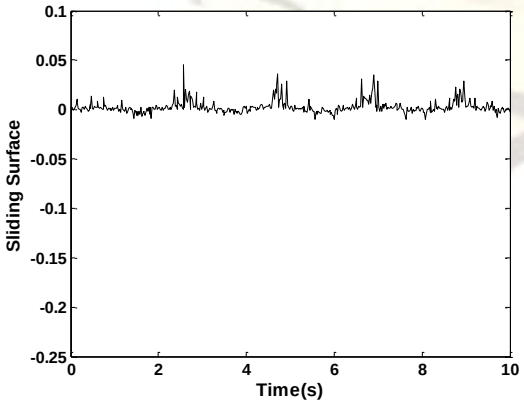

Fig.7 Sliding surface

Fig. 8 shows controller u_1 versus time. Fig. 9 shows controller u_2 versus time. Fig. 10 presents control law u of mobile inverted pendulum to track reference.

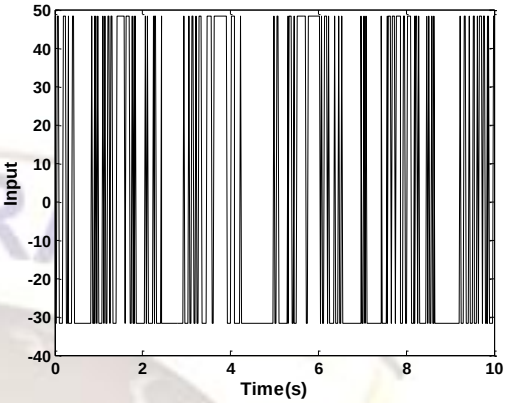

Fig. 8 Dynamic controller u_1

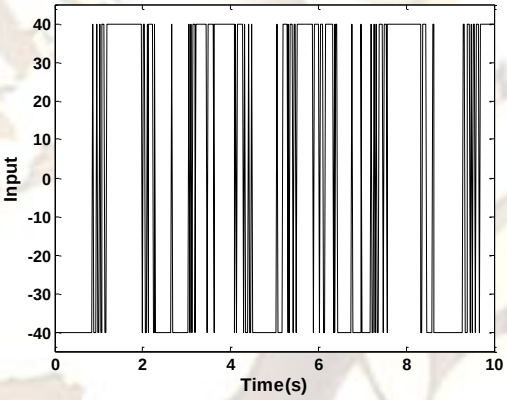

Fig. 9 Dynamic controller u_2

The experimental results in stable condition are given after errors converge through Figs.(11) ~ (13). The encoder voltage is shown in Fig. 11. Fig. 12 presents the output voltage of tilt sensor. Fig. 13 presents motor PWM output under the proposed controller u in experiment.

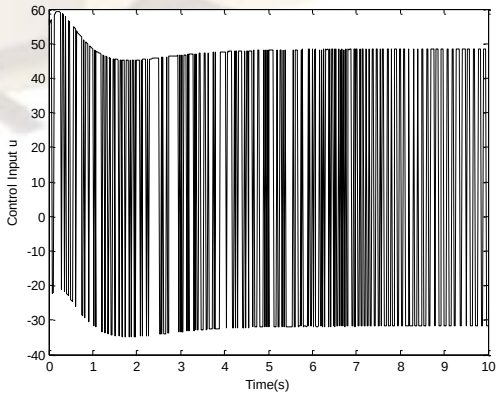

Fig. 10 Controller input u

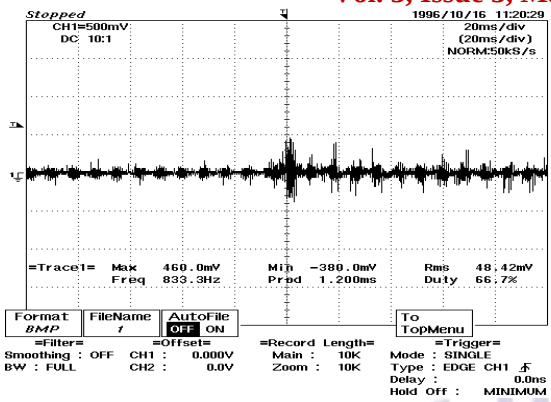

Fig. 11 Output voltage of motor encoder

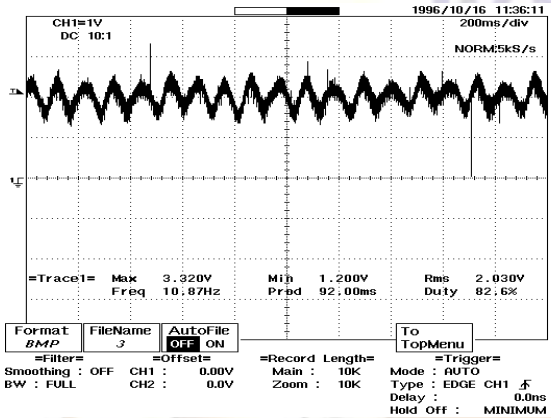

Fig. 12 Output voltage of tilt sensor

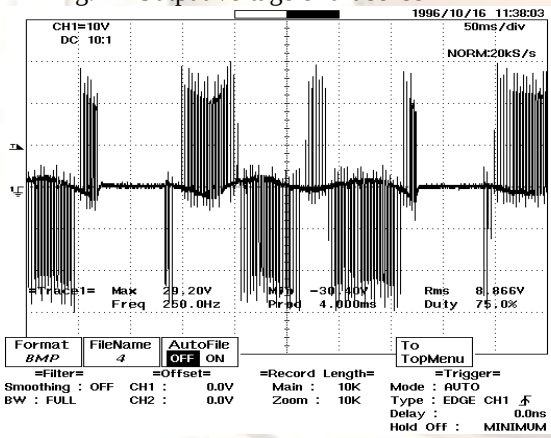

Fig. 13 PWM output of DC motor under control law

6 Conclusion

This paper presents a sliding mode tracking controller for the mobile inverted pendulum. The controller is developed based upon a class of nonlinear systems whose nonlinear part of the modeling can be linearly parameterized. The tracking errors are defined, and then the sliding surface is chosen in an explicit form using Ackermann's formula to guarantee that the tracking error converge to zero asymptotically.

The simulation and experimental results show that the proposed controller is applicable and implemented in the practical field.

REFERENCES:

[1] F. Grasser, A. D'Arrigo, S. Colombi and A. C. Rufer, JOE: a Mobile, Inverted Pendulum, IEEE Trans. Industrial Electronics, Vol. 49, No. 1(2002), pp. 107~114.

[2] C.S. Chen and W.L. Chen: Robust Adaptive Sliding-mode Control Using Fuzzy Modeling for an Inverted-pendulum System, IEEE Trans. Industrial Electronics, Vol. 45, No. 2(1998), pp. 297~306.

[3] S.J. Huang and C.L. Huang: Control of an Inverted Pendulum Using Grey Prediction Model, IEEE Trans. Industrial Applications, Vol. 36, No. 2(2000), pp. 452~458.

[4] J. Ackermann and V. Utkin: Sliding Mode Control Design Based on Ackermann's Formula, IEEE Trans. Automatic Control, Vol. 43, No. 2(1998), pp. 234~237.

[5] D. Necsulescu: Mechatronics, Prentice-Hall, Inc. (2002), pp. 57~60.

[6] M.T. Kang: M.S. Thesis, Control for Mobile Inverted Pendulum Using Sliding Mode Technique, Pukyong National University, (2007).

Appendix A

Nomenclature

Variable	Description	Units
V	Motor voltage	V
i	Current armature	A
ω	Rotor angular velocity	rad/s
V_e	Back electromotive force voltage	V
K_e	Back electromotive voltage coefficient	Vs/rad
I_R	Inertia moment of the rotor	$Kg \cdot m^2$
T_m	Magnetic torque of the rotor	Nm
K_m	Magnetic torque coefficient	Nm/A
T	Load torque of the motor	Nm
K_f	Viscous frictional coefficient of rotor shaft	Nms/rad
R	Nominal rotor resistance	Ω
H	Nominal rotor inductance	H
x_c	Cart position perpendicular to the wheel axis	m
φ	Inverted pendulum angle	rad
φ_d	Desired inverted pendulum angle	rad
L	Distance between the wheel axis and the pendulum's center	m
D	Lateral distance between two coaxial wheels	m

T_L, T_R	Torques acting on the left and the right wheel	Nm
H_L, P_L	Reaction force between left wheel and the inverted pendulum	N
H_R, P_R	Reaction force between right wheel and the inverted pendulum	N
θ_{Lw}, θ_{Rw}	Rotation angles of the left and right wheel	rad
x_L, x_R	left and right wheel position	m
H_{fL}, H_{fR}	Friction forces between the left and right wheel and the ground	N
r	Wheel radius	m
M_p	Pendulum mass	Kg
I_p	Inertia moment of the inverted pendulum around the wheel axis	$Kg \cdot m^2$
M_w	Wheel mass with DC motor	Kg
I_w	Inertia moment of wheel with rotor around the wheel axis	$Kg \cdot m^2$
g	Gravitation acceleration	m/s^2

Appendix B

$$a_{22} = -\frac{2K_m K_e (M_p L r + I_p + M_p L^2)}{R r^2 \alpha},$$

$$a_{23} = \frac{M_p^2 g L^2}{\alpha},$$

$$a_{42} = \frac{2K_m K_e (r\beta + M_p L)}{R r^2 \alpha},$$

$$a_{43} = -\frac{M_p g L \beta}{\alpha},$$

$$b_2 = \frac{2K_m (I_p + M_p L^2 + M_p L r)}{R r \alpha},$$

$$b_4 = -\frac{2K_m (M_p L + r\beta)}{R r \alpha},$$

where $\beta = (2M_w + \frac{2I_w}{r^2} + M_p)$,

$$\alpha = \left[I_p \beta + 2M_p L^2 (M_w + \frac{I_w}{r^2}) \right].$$

Appendix C

$$A - bk^T = \begin{bmatrix} a_{11} & a_{12} & a_{13} & a_{14} \\ a_{21} & a_{22} & a_{23} & a_{24} \\ a_{31} & a_{32} & a_{33} & a_{34} \\ a_{41} & a_{42} & a_{43} & a_{44} \end{bmatrix} - \begin{bmatrix} b_1k_1 & b_1k_2 & b_1k_3 & b_1k_4 \\ b_2k_1 & b_2k_2 & b_2k_3 & b_2k_4 \\ b_3k_1 & b_3k_2 & b_3k_3 & b_3k_4 \\ b_4k_1 & b_4k_2 & b_4k_3 & b_4k_4 \end{bmatrix} \quad \text{(C1)}$$

$$= \begin{bmatrix} a_{11} - b_1k_1 & a_{12} - b_1k_2 & a_{13} - b_1k_3 & a_{14} - b_1k_4 \\ a_{21} - b_2k_1 & a_{22} - b_2k_2 & a_{23} - b_2k_3 & a_{24} - b_2k_4 \\ a_{31} - b_3k_1 & a_{32} - b_3k_2 & a_{33} - b_3k_3 & a_{34} - b_3k_4 \\ a_{41} - b_4k_1 & a_{42} - b_4k_2 & a_{43} - b_4k_3 & a_{44} - b_4k_4 \end{bmatrix} = \begin{bmatrix} A_{11} & A_{12} & A_{13} & A_{14} \\ A_{21} & A_{22} & A_{23} & A_{24} \\ A_{31} & A_{32} & A_{33} & A_{34} \\ A_{41} & A_{42} & A_{43} & A_{44} \end{bmatrix}$$

$$\bar{A} = T(A - bk^T)T^{-1} = \begin{bmatrix} 1 & 0 & 0 & 0 \\ 0 & 1 & 0 & 0 \\ 0 & 0 & 1 & 0 \\ c_1 & c_2 & c_3 & c_4 \end{bmatrix} \begin{bmatrix} A_{11} & A_{12} & A_{13} & A_{14} \\ A_{21} & A_{22} & A_{23} & A_{24} \\ A_{31} & A_{32} & A_{33} & A_{34} \\ A_{41} & A_{42} & A_{43} & A_{44} \end{bmatrix} \begin{bmatrix} 1 & 0 & 0 & 0 \\ 0 & 1 & 0 & 0 \\ 0 & 0 & 1 & 0 \\ -\frac{c_1}{c_4} & -\frac{c_2}{c_4} & -\frac{c_3}{c_4} & \frac{1}{c_4} \end{bmatrix}$$

$$= \left[\begin{array}{ccc:c} A_{11} - A_{14}\frac{c_1}{c_4} & A_{12} - A_{14}\frac{c_2}{c_4} & A_{13} - A_{14}\frac{c_3}{c_4} & \frac{A_{14}}{c_4} \\ A_{21} - A_{24}\frac{c_1}{c_4} & A_{22} - A_{24}\frac{c_2}{c_4} & A_{23} - A_{24}\frac{c_3}{c_4} & \frac{A_{24}}{c_4} \\ A_{31} - A_{34}\frac{c_1}{c_4} & A_{32} - A_{34}\frac{c_2}{c_4} & A_{33} - A_{34}\frac{c_3}{c_4} & \frac{A_{34}}{c_4} \\ \hdashline Q_1 - Q_4\frac{c_1}{c_4} & Q_2 - Q_4\frac{c_2}{c_4} & Q_3 - Q_4\frac{c_3}{c_4} & \frac{Q_4}{c_4} \end{array}\right] \quad \text{(C2)}$$

where

$$Q_1 = c_1A_{11} + c_2A_{21} + c_3A_{31} + c_4A_{41} \quad \text{(C3)}$$

$$Q_2 = c_1A_{12} + c_2A_{22} + c_3A_{32} + c_4A_{42}$$

$$Q_3 = c_1A_{13} + c_2A_{23} + c_3A_{33} + c_4A_{43}$$

$$Q_4 = c_1A_{14} + c_2A_{24} + c_3A_{34} + c_4A_{44}.$$

From (21), (C1) and (C3), the followings can be obtained

$$Q \equiv \begin{bmatrix} Q_1 & Q_2 & Q_3 & Q_4 \end{bmatrix} = C^T \left(A - bk^T \right)$$

$$= C^T\lambda_4 = \begin{bmatrix} c_1\lambda_4 & c_2\lambda_4 & c_3\lambda_4 & c_4\lambda_4 \end{bmatrix} \quad \text{(C4)}$$

$$Q_1 - Q_4\frac{c_1}{c_4} = c_1\lambda_4 - c_4\lambda_4\frac{c_1}{c_4} = 0$$

$$Q_2 - Q_4\frac{c_2}{c_4} = c_2\lambda_4 - c_4\lambda_4\frac{c_2}{c_4} = 0$$

$$Q_3 - Q_4\frac{c_3}{c_4} = c_3\lambda_4 - c_4\lambda_4\frac{c_3}{c_4} = 0$$

$$\frac{Q_4}{c_4} = \frac{c_4\lambda_4}{c_4} = \lambda_4 \quad \text{(C5)}$$

Substituting (C5) into (C2) can be rewritten as follows:

$$\bar{A} = \left[\begin{array}{ccc:c} A_{11} - A_{14}\frac{c_1}{c_4} & A_{12} - A_{14}\frac{c_2}{c_4} & A_{13} - A_{14}\frac{c_3}{c_4} & \frac{A_{14}}{c_4} \\ A_{21} - A_{24}\frac{c_1}{c_4} & A_{22} - A_{24}\frac{c_2}{c_4} & A_{23} - A_{24}\frac{c_3}{c_4} & \frac{A_{24}}{c_4} \\ A_{31} - A_{34}\frac{c_1}{c_4} & A_{32} - A_{34}\frac{c_2}{c_4} & A_{33} - A_{34}\frac{c_3}{c_4} & \frac{A_{34}}{c_4} \\ \hdashline 0 & 0 & 0 & \lambda_4 \end{array}\right] = \begin{bmatrix} A_1 & a_1 \\ 0 & \lambda_4 \end{bmatrix}$$